

Received February 1, 2021, accepted March 23, 2021, date of publication March 30, 2021, date of current version April 6, 2021.

Digital Object Identifier 10.1109/ACCESS.2021.3069327

Height Measurement With Meter Wave MIMO Radar Based on Precise Signal Model Under Complex Terrain

YUWEI SONG, GUOPING HU, AND GUIMEI ZHENG 

Air Force Engineering University, Xi'an 710051, China

Corresponding author: Guimei Zheng (zheng-gm@163.com)


This work was supported in part by the Young Talent Fund of University Association for Science and Technology in Shaanxi of China under Grant 20180109, in part by the Natural Science Basic Research Plan in Shaanxi Province of China under Grant 2019JM-155, and in part by the National Natural Science Foundation of China under Grant 61971438.

ABSTRACT Meter wave radar height measurement is one of the most difficult problems in meter wave radar system. At present, the most popular height measurement methods of meter wave radar include beam splitting method, MUSIC algorithm and maximum likelihood estimation method, which can achieve good performance under flat ground. However, the real ground is not ideal condition, and the situation of undulating ground is also very complicated. Under this condition, the performance of the above algorithm dropped sharply. Many researchers solve this problem by improving the robustness of the algorithm. However, the authors think that the key to solve the problem is to establish a refined height measurement signal model. In this paper, the accurate model of reflection coefficient, reflection height and reflection point under the condition of undulating ground are established to provide accurate signal model for meter wave radar height measurement. Then we deduce the application of generalized MUSIC algorithm and maximum likelihood estimation algorithm for MIMO radar in the accurate terrain signal model. In fact, the method proposed in this paper is a terrain matching MIMO radar target height measurement, and the traditional algorithm can be regarded as terrain mismatch. The simulation results show that the accuracy of terrain matching estimation of the precise signal model established in this paper is much better than that of the traditional simplified signal model.

INDEX TERMS MIMO radar, height measurement, meter wave radar, precise signal model.

I. INTRODUCTION

With the development of stealth technology, meter wave radar has ushered in World War II because of its strong anti stealth ability. Direction of arrival (DOA) estimation has always been one of the hotspots in radar field. Therefore, many scholars began to pay attention to the meter wave radar angle estimation problem, at this time the meter wave radar low elevation angle estimation problem appeared in people's field of vision. Meter wave radar has a wide beam and low band [1], [2], and there is multipath effect in low elevation area, which means that direct wave and reflected wave are regarded as a group of coherent signals. After a long period of research, the conventional meter wave array radar has been developed more mature and has many achievements.

The associate editor coordinating the review of this manuscript and approving it for publication was Jing Liang .

In low elevation measurement, a suitable signal model is very important. Reference [3] proposed a low elevation height measurement method based on lobes beam splitting due to ground reflection with wide beam width of meter wave radar. Its signal model is an ideal reflection signal model, and the height measurement accuracy will drop sharply when the terrain is not flat in reality. A generalized MUSIC algorithm is proposed in Reference [4]. The algorithm can measure the elevation angle of target under multipath interference without decoherence processing, and has good angle measurement accuracy. However, its signal model is still an ideal reflection model, and its height measurement accuracy will still decline once it is in complex terrain. In order to solve the problem of mismatching with the actual signal model, Reference [5] derived a meter wave radar multipath signal model under complex terrain, and proposed a new height estimation method based on alternating projection. The algorithm

considers the influence of complex terrain on low elevation angle height measurement, and reduces the complexity of the algorithm. In Reference [6], a low elevation angle estimation method for wide band radar based on super-resolution algorithm is proposed, which is more suitable for complex terrain than conventional narrow-band radar low elevation estimation method.

As we all know, MIMO has the advantage of waveform diversity. In parameter estimation, larger virtual aperture can be obtained to improve the accuracy of angle estimation [7]–[10]. Therefore, the low elevation angle estimation of meter wave MIMO array radar has been widely studied. The echo capability superposition method can improve the height measurement accuracy of distributed MIMO radar [11], [12]. Height measurement of distributed MIMO radar is not the focus of this paper, and will not be discussed here. For co-located meter wave MIMO array radar, height measurement methods include maximum likelihood [13], [14], generalized MUSIC [15], intelligent algorithm [16], [17], beam splitting algorithm [18], time reversal and other technologies [19]. These methods can solve the problem of meter wave MIMO radar height measurement. In addition, due to the high degree of freedom and large amount of computation of MIMO array radar, the methods of beam space, matrix beam and dimension reduction root reduction are proposed in the References [20], [21] to reduce the calculation amount, which have achieved good height measurement results. However, the reflection point on complex terrain in References [13]–[22] is only located into one point, and the reflection coefficients of all elements are the same values, which is seriously inconsistent with the actual signal model.

In order to match the actual situation, a new complex terrain signal model is proposed in this paper, which considers the reflection points of each element in the array are in different positions. In this signal model, the reflection points of each element are different, and the reflection coefficient is also different due to different reflection points. Firstly, the situation of considering each element’s reflection point under flat ground is deduced. Then, the traditional height measurement model of undulating ground is briefly reviewed. Then, the height measurement model of undulating ground considering each element and each signal reflection point is derived. Through theoretical derivation, the signal model is close to the actual signal model. Finally, aiming at the accurate terrain signal model, this paper deduces the application of maximum likelihood method and generalized MUSIC method in MIMO radar. This work appeared in part in the Reference [23].

II. HEIGHT MEASUREMENT SIGNAL MODEL OF FLAT GROUND

Consider an isotropic radar system with the highest element as a reference, and its transmit signal is set to $s(t)$. It is assumed that the gain and characteristics of the receiving elements are the same, and the channel consistency is good. The signal receiving schematic diagram of classical flat ground

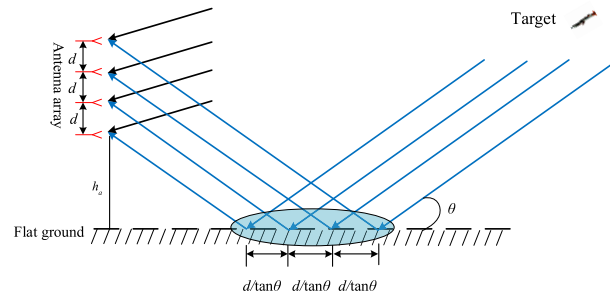


FIGURE 1. Model of reflected signal of flat ground.

is shown in Figure 1. Notice: in this paper, Signal transmission is assumed to be non-attenuated, only the phase change caused by delay.

Then the direct wave signal received by the reference array element is:

$$s(t)e^{-j2\pi f \frac{R_{d,1}}{c}}, \quad R_{d,1} = \sqrt{(h_t - h_1)^2 + R^2} \approx \bar{R} - h_1 \sin \theta_d \quad (1)$$

where \bar{R} is the slant distance between the radar and the target, c represents the speed of light, and f represents the operating frequency of the radar, which is set to 300MHz in this paper. Among them, the antenna height equals $h_1 = h_a + (N - 1)d$. h_a is the height of the lowest antenna element of the antenna, d is the distance between the elements with equal spacing, N is the total number of array elements, R is the horizontal distance of the projection of the antenna array and the target on the horizontal plane, $R_{d,1}$ is the wave path from the target to the reference array element, and h_t is the height from the target to the horizontal plane. θ_d is the target angle of the direct wave.

The direct wave signal of the second array element from top to bottom is:

$$s(t)e^{-j2\pi f \frac{R_{d,2}}{c}}, \quad R_{d,2} = \sqrt{(h_t - h_2)^2 + R^2} \approx \bar{R} - h_2 \sin \theta_d \quad (2)$$

The direct wave signal of the N -th element is:

$$s(t)e^{-j2\pi f \frac{R_{d,N}}{c}}, \quad R_{d,N} = \sqrt{(h_t - h_N)^2 + R^2} \approx \bar{R} - h_N \sin \theta_d \quad (3)$$

Therefore, the direct wave signal vector can be written as:

$$\begin{aligned} \mathbf{x}_d(t) &= \left[s(t)e^{-j2\pi f \frac{R_{d,1}}{c}}, s(t)e^{-j2\pi f \frac{R_{d,2}}{c}}, \dots, s(t)e^{-j2\pi f \frac{R_{d,N}}{c}} \right]^T \\ &= s(t)e^{-j2\pi f \frac{\bar{R}}{c}} \left[e^{j2\pi f \frac{h_1 \sin \theta_d}{c}}, e^{j2\pi f \frac{h_2 \sin \theta_d}{c}}, \dots, e^{-j2\pi f \frac{h_N \sin \theta_d}{c}} \right]^T \\ &= s(t)e^{-j2\pi f \frac{\bar{R} - (h_a + (N-1)d) \sin \theta_d}{c}} \\ &\quad \times \left[1, e^{-j2\pi f \frac{d \sin \theta_d}{c}}, \dots, e^{-j2\pi f \frac{(N-1)d \sin \theta_d}{c}} \right]^T \end{aligned}$$

$$\begin{aligned}
 &= s(t)e^{-j2\pi f \frac{R_{d,1}}{c}} \left[1, e^{-j2\pi f \frac{d \sin \theta_d}{c}}, \dots, e^{-j2\pi f \frac{(N-1)d \sin \theta_d}{c}} \right]^T \\
 &= s(t)e^{-j2\pi f \frac{R_{d,1}}{c}} \mathbf{a}(\theta_d) \tag{4}
 \end{aligned}$$

Next, the reflected wave signal received by the reference array element is deduced as follows:

$$\begin{aligned}
 \rho_1 s(t)e^{-j2\pi f \frac{R_{s,1}}{c}}, \quad R_{s,1} &= \sqrt{(h_t + h_1)^2 + R^2} \\
 &\approx \bar{R} + h_1 \sin \theta_s \\
 &= R_{d,1} + \Delta R_1 \tag{5}
 \end{aligned}$$

θ_s is the angle of the target reflected wave. ΔR_1 is the wave path difference between the direct wave and the reflected wave, which is equal to $\Delta R_1 = 2 \frac{h_1 h_t}{R}$.

The reflected wave signal received by the second element is:

$$\rho_2 s(t)e^{-j2\pi f \frac{R_{s,2}}{c}}, \quad R_{s,2} = \sqrt{(h_t + h_2)^2 + R^2} \approx \bar{R} + h_2 \sin \theta_s \tag{6}$$

The reflected wave signal received by the N -th element is:

$$\begin{aligned}
 \rho_N s(t)e^{-j2\pi f \frac{R_{s,N}}{c}}, \quad R_{s,N} &= \sqrt{(h_t + h_N)^2 + R^2} \\
 &\approx \bar{R} + h_N \sin \theta_s \tag{7}
 \end{aligned}$$

Therefore, the reflected wave signal vector can be written as follows:

$$\begin{aligned}
 \mathbf{x}_s(t) &= \left[\rho_1 s(t)e^{-j2\pi f \frac{R_{s,1}}{c}}, \rho_2 s(t)e^{-j2\pi f \frac{R_{s,2}}{c}}, \dots, \rho_N s(t)e^{-j2\pi f \frac{R_{s,N}}{c}} \right]^T \\
 &= s(t)e^{-j2\pi f \frac{\bar{R}}{c}} \\
 &\quad \left[\rho_1 e^{j2\pi f \frac{-h_1 \sin \theta_s}{c}}, \rho_2 e^{j2\pi f \frac{-h_2 \sin \theta_s}{c}}, \dots, \rho_N e^{-j2\pi f \frac{-h_N \sin \theta_s}{c}} \right]^T \\
 &= s(t)e^{-j2\pi f \frac{\bar{R} + (h_t + (N-1)d) \sin \theta_s}{c}} \\
 &\quad \left[\rho_1, \rho_2 e^{-j2\pi f \frac{d \sin \theta_s}{c}}, \dots, \rho_N e^{-j2\pi f \frac{(N-1)d \sin \theta_s}{c}} \right]^T \\
 &= s(t)e^{-j2\pi f \frac{R_{s,1}}{c}} \boldsymbol{\rho} \odot \left[1, e^{-j2\pi f \frac{d \sin \theta_s}{c}}, \dots, e^{-j2\pi f \frac{(N-1)d \sin \theta_s}{c}} \right]^T \\
 &= s(t)e^{-j2\pi f \frac{R_{s,1}}{c}} \boldsymbol{\rho} \odot \mathbf{a}(\theta_s) \tag{8}
 \end{aligned}$$

Then the received data of the whole array is:

$$\begin{aligned}
 \mathbf{x}(t) &= \mathbf{x}_d(t) + \mathbf{x}_s(t) + \mathbf{n}(t) \\
 &= s(t)e^{-j2\pi f \frac{R_{d,1}}{c}} \mathbf{a}(\theta_d) + s(t)e^{-j2\pi f \frac{R_{s,1}}{c}} \boldsymbol{\rho} \odot \mathbf{a}(\theta_s) + \mathbf{n}(t) \\
 &= \left[\mathbf{a}(\theta_d) + e^{-j2\pi f \frac{R_{s,1} - R_{d,1}}{c}} \boldsymbol{\rho} \odot \mathbf{a}(\theta_s) \right] s(t)e^{-j2\pi f \frac{R_{d,1}}{c}} + \mathbf{n}(t) \\
 &= \left[\mathbf{a}(\theta_d) + e^{-j2\pi f \frac{2h_1 h_t}{cR}} \boldsymbol{\rho} \odot \mathbf{a}(\theta_s) \right] s(t)e^{-j2\pi f \frac{R_{d,1}}{c}} + \mathbf{n}(t) \tag{9}
 \end{aligned}$$

It is noted that the inconsistency between the signal model of the above-mentioned flat ground and the traditional signal model is the reflection coefficient, which is a vector, while the traditional reflection coefficient is regarded as a scalar, that is, the ground of the reflection point is generally regarded

as a reflection point, as shown in Figure 2. Then the reflection coefficient is $[\rho_1 = \rho_2 = \dots = \rho_N = \rho]$. In fact, it is simplified here. It can be seen that the distance between the reflection points is $\frac{d}{\tan \theta_s}$, assuming $d = 1$ m, $\theta_s = 2^\circ$, the distance between adjacent reflection points is 28.6 m. It can be seen that the distance between the reflection points is relatively large. Thus, when the ground medium is not uniform, it is not accurate to set the reflection coefficient of the traditional algorithm to a value, which will affect the height measurement effect.

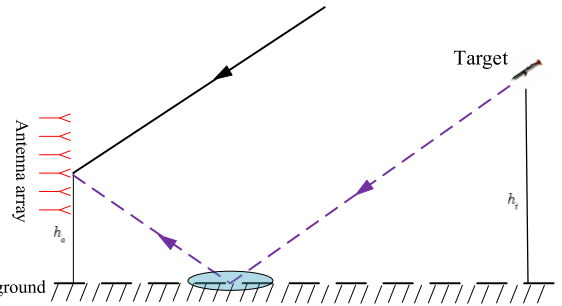


FIGURE 2. Model of reflected signal from flat ground - simplified version.

III. TRADITIONAL HEIGHT MEASUREMENT MODEL OF UNDULATING GROUND

Firstly, the signal model of traditional undulating ground is introduced, and it is considered that there is only one undulating reflection point, which is equivalent to making two assumptions in the algorithm: one is that the reflection point is only concentrated in one physical geometric point; secondly, it is considered that the undulating reflection point has only one value, which is equivalent to the simplified signal model of undulating ground, as shown in Figure 3.

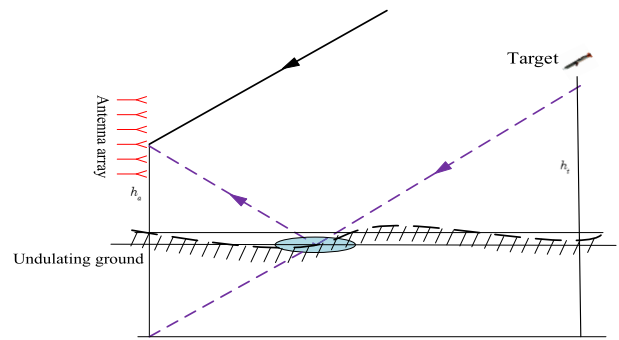


FIGURE 3. Reflected signal model of undulating ground-simplified version.

For the undulating ground model, the received signal of direct wave is consistent with the flat ground

$$\mathbf{x}_d(t) = s(t)e^{-j2\pi f \frac{R_{d,1}}{c}} \mathbf{a}(\theta_d) \tag{10}$$

For the reflected signal, it needs to be determined according to the undulating ground, and the reflection points corresponding to multiple array elements are reduced to the same

reflection point. Therefore, first of all, we need to define the height of the reflection point h_s , and define the reflection point as a negative number above the ground level. The reflection point is a positive number if it is below the ground level. Therefore, we can see that the height of the reflection point is $h_a + h_s$, which h_a is the height of the antenna (in fact, in this simplified model, previous literatures and algorithms do not know exactly). Then the horizontal distance of the reflection point is $(h_a + h_s)\tan(\theta_s)$, the calculation of the reflection coefficient needs to use the dielectric constant and conductivity of the point. The signal model of reflected wave is derived as follows:

The reflected wave signal of the i -th element is:

$$\rho_i s(t) e^{-j2\pi f \frac{\bar{R}_{s,i}}{c}}, \quad \bar{R}_{s,i} = \sqrt{(h_t + h_i + 2h_{s,i})^2 + R^2} \approx \bar{R} + (h_i + 2h_{s,i}) \sin \theta_s \quad (11)$$

It should be emphasized that the reflection coefficient is set to a value, that is $[\rho_1 = \rho_2 = \dots = \rho_N = \rho]$, the fluctuation of reflection points is reduced to a value, i.e. $[h_{s,1} = h_{s,2} = \dots = h_{s,N} = h_s]$. Therefore, the reflected signal vector of the whole array is:

$$\begin{aligned} \mathbf{x}_{s, \text{coarse}}(t) &= \left[\rho s(t) e^{-j2\pi f \frac{\bar{R}_{s,1}}{c}}, \rho s(t) e^{-j2\pi f \frac{\bar{R}_{s,2}}{c}}, \dots, \rho s(t) e^{-j2\pi f \frac{\bar{R}_{s,N}}{c}} \right]^T \\ &= \rho s(t) e^{-j2\pi f \frac{\bar{R}}{c}} \left[e^{j2\pi f \frac{-(h_1+2h_s) \sin \theta_s}{c}}, e^{j2\pi f \frac{-(h_2+2h_s) \sin \theta_s}{c}}, \dots, e^{-j2\pi f \frac{-(h_N+2h_s) \sin \theta_s}{c}} \right]^T \\ &= \rho s(t) e^{-j2\pi f \frac{\bar{R}+(h_1+2h_s) \sin \theta}{c}} \times \left[1, e^{-j2\pi f \frac{d \sin \theta_s}{c}}, \dots, e^{-j2\pi f \frac{(N-1)d \sin \theta_s}{c}} \right]^T \\ &= \rho s(t) e^{-j2\pi f \frac{\bar{R}+(h_1+2h_s) \sin \theta}{c}} \times \left[1, e^{-j2\pi f \frac{d \sin \theta_s}{c}}, \dots, e^{-j2\pi f \frac{(N-1)d \sin \theta_s}{c}} \right]^T \\ &= \rho s(t) e^{-j2\pi f \frac{\bar{R}+(h_1+2h_s) \sin \theta_s}{c}} \mathbf{a}(\theta_s) \quad (12) \end{aligned}$$

Therefore, the received data of direct wave plus reflected wave of the whole array are as follows:

$$\begin{aligned} \mathbf{x}(t) &= \mathbf{x}_d(t) + \mathbf{x}_{s, \text{coarse}}(t) + \mathbf{n}(t) \\ &= s(t) e^{-j2\pi f \frac{R_{d,1}}{c}} \mathbf{a}(\theta_d) + s(t) e^{-j2\pi f \frac{\bar{R}+(h_1+2h_s) \sin \theta_s}{c}} \rho \mathbf{a}(\theta_s) + \mathbf{n}(t) \\ &= \left[\mathbf{a}(\theta_d) + e^{-j2\pi f \frac{\bar{R}+(h_1+2h_s) \sin \theta_s - R_{d,1}}{c}} \rho \mathbf{a}(\theta_s) \right] s(t) e^{-j2\pi f \frac{R_{d,1}}{c}} + \mathbf{n}(t) \\ &= \left[\mathbf{a}(\theta_d) + e^{-j2\pi f \frac{2h_1 h_t}{cR}} \rho \mathbf{a}(\theta_s) \right] s(t) e^{-j2\pi f \frac{R_{d,1}}{c}} + \mathbf{n}(t) \quad (13) \end{aligned}$$

IV. REFINED HEIGHT MEASUREMENT MODEL PROPOSED IN THIS PAPER

In fact, target is not on the same horizontal line as the array antenna; secondly, reflection points are not on the unified horizontal line, that is, the height of reflection points are not

equal, and the grounds of the reflection points are inconsistent. The refined structure of the reflected signal model of the undulating ground is shown in Figure 4. Next, we derive the refined signal model and calculate the ground of the reflection point according to the height of the reflection point.

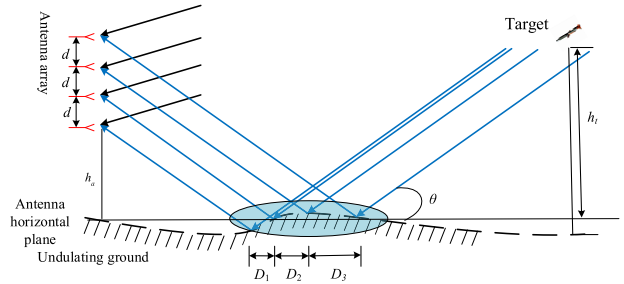


FIGURE 4. Reflected signal model of undulating ground-fine version.

First of all, it can be seen from Figure 4 that the wave path of the direct wave using the existing algorithm is different from that of the traditional algorithm, because the information h_t to be used is the height from the target to the antenna horizontal plane. It should be noted that there are two types of radar height measurement, one is the relative height of the target, which is referred to in this paper h_t , and the other is to add the altitude on the basis of h_t . But the height of the target to the ground surface is never used in radar engineering.

We can see that the reflection points are not evenly distributed, that is, D_1, D_2, D_3 are not equal. Next, the signal model is deduced in detail.

The direct wave signal received by the reference array element is:

$$s(t) e^{-j2\pi f \frac{\bar{R}_{d,1}}{c}}, \quad \bar{R}_{d,1} = \sqrt{(h_t - h_1)^2 + R^2} \approx \bar{R} - h_1 \sin \theta_d \quad (14)$$

The direct wave signal received by the second array is:

$$s(t) e^{-j2\pi f \frac{\bar{R}_{d,2}}{c}}, \quad \bar{R}_{d,2} = \sqrt{(h_t - h_2)^2 + R^2} \approx \bar{R} - h_2 \sin \theta_d \quad (15)$$

The direct wave signal received by the N th array is:

$$s(t) e^{-j2\pi f \frac{\bar{R}_{d,N}}{c}}, \quad \bar{R}_{d,N} = \sqrt{(h_t - h_N)^2 + R^2} \approx \bar{R} - h_N \sin \theta_d \quad (16)$$

Therefore, the direct wave signal vector can be written as:

$$\begin{aligned} \bar{\mathbf{x}}_d(t) &= \left[s(t) e^{-j2\pi f \frac{\bar{R}_{d,1}}{c}}, s(t) e^{-j2\pi f \frac{\bar{R}_{d,2}}{c}}, \dots, s(t) e^{-j2\pi f \frac{\bar{R}_{d,N}}{c}} \right]^T \\ &= s(t) e^{-j2\pi f \frac{\bar{R} \sin \theta_d}{c}} \times \left[e^{-j2\pi f \frac{h_1 \sin \theta_d}{c}}, e^{-j2\pi f \frac{h_2 \sin \theta_d}{c}}, \dots, e^{-j2\pi f \frac{h_N \sin \theta_d}{c}} \right]^T \\ &= s(t) e^{-j2\pi f \frac{\bar{R}+h_1 \sin \theta_d}{c}} \left[1, e^{-j2\pi f \frac{d \sin \theta_d}{c}}, \dots, e^{-j2\pi f \frac{(N-1)d \sin \theta_d}{c}} \right]^T \end{aligned}$$

$$\begin{aligned}
 &= s(t)e^{-j2\pi f \frac{\bar{R}_{d,1}}{c}} \left[1, e^{-j2\pi f \frac{d \sin \theta_d}{c}}, \dots, e^{-j2\pi f \frac{(N-1)d \sin \theta_d}{c}} \right]^T \\
 &= s(t)e^{-j2\pi f \frac{\bar{R}_{d,1}}{c}} \mathbf{a}(\theta_d) \tag{17}
 \end{aligned}$$

The reflected wave signal received by the reference array element is:

$$\begin{aligned}
 \rho_1 s(t)e^{-j2\pi f \frac{\bar{R}_{s,1}}{c}}, \quad \bar{R}_{s,1} &= \sqrt{(h_t + (h_1 + 2h_{s,1}))^2 + R^2} \\
 &\approx \bar{R} + (h_1 + 2h_{s,1}) \sin \theta_s \\
 &= \bar{R}_{d,1} + \Delta R_1 \tag{18}
 \end{aligned}$$

Wave path difference between the direct and reflected wave equals $\Delta R_1 = 2 \frac{(h_1 + 2h_{s,1})h_t}{R}$, $h_t - h_1 = R \tan \theta_d$, $h_t + h_1 = R \tan \theta_s$.

The reflected wave signal received by the second array element is:

$$\begin{aligned}
 \rho_2 s(t)e^{-j2\pi f \frac{\bar{R}_{s,2}}{c}}, \quad \bar{R}_{s,2} &= \sqrt{(h_t + (h_2 + 2h_{s,2}))^2 + R^2} \\
 &\approx \bar{R} + (h_2 + 2h_{s,2}) \sin \theta_s \\
 &= R_{d,2} + 2 \frac{(h_2 + 2h_{s,2})h_t}{R} \tag{19}
 \end{aligned}$$

The reflected wave signal of the N element is:

$$\begin{aligned}
 \rho_N s(t)e^{-j2\pi f \frac{\bar{R}_{s,N}}{c}}, \quad \bar{R}_{s,N} &= \sqrt{(h_t + (h_N + 2h_{s,N}))^2 + R^2} \\
 &\approx \bar{R} + (h_N + 2h_{s,N}) \sin \theta_s \\
 &= R_{d,N} + 2 \frac{(h_N + 2h_{s,N})h_t}{R} \tag{20}
 \end{aligned}$$

Therefore, the reflected wave signal vector can be written as follows:

$$\begin{aligned}
 \bar{\mathbf{x}}_s(t) &= \left[\rho_1 s(t)e^{-j2\pi f \frac{\bar{R}_{s,1}}{c}}, \dots, \rho_N s(t)e^{-j2\pi f \frac{\bar{R}_{s,N}}{c}} \right]^T \\
 &= s(t)e^{-j2\pi f \frac{\bar{R}}{c}} \left[\rho_1 e^{j2\pi f \frac{-(h_1 + 2h_{s,1}) \sin \theta_s}{c}}, \dots, \rho_N e^{j2\pi f \frac{-(h_N + 2h_{s,N}) \sin \theta_s}{c}} \right]^T \\
 &= s(t)e^{-j2\pi f \frac{\bar{R} + h_1 \sin \theta_s}{c}} \\
 &\quad \times \left[\rho_1 e^{j2\pi f \frac{-2h_{s,1} \sin \theta_s}{c}}, \dots, \rho_N e^{j2\pi f \frac{-2h_{s,N} \sin \theta_s}{c}} e^{-j2\pi f \frac{(N-1)d \sin \theta_s}{c}} \right]^T \\
 &= s(t)e^{-j2\pi f \frac{\bar{R} + h_1 \sin \theta_s}{c}} \\
 &\quad \times \left[\rho_1 e^{j2\pi f \frac{-2h_{s,1} \sin \theta_s}{c}}, \dots, \rho_N e^{j2\pi f \frac{-2h_{s,N} \sin \theta_s}{c}} e^{-j2\pi f \frac{(N-1)d \sin \theta_s}{c}} \right]^T \tag{21}
 \end{aligned}$$

where

$$\boldsymbol{\rho}(h_{s,i}) = [\rho_1(h_{s,1}), \rho_2(h_{s,2}), \dots, \rho_N(h_{s,N})]^T \tag{22}$$

$$\mathbf{a}_{\text{terrain}}(h_{s,i}) = \left[e^{j2\pi f \frac{-2h_{s,1} \sin \theta_s}{c}}, \dots, e^{j2\pi f \frac{-2h_{s,N} \sin \theta_s}{c}} \right]^T \tag{23}$$

$$\bar{\mathbf{x}}_s(t) = s(t)e^{-j2\pi f \frac{\bar{R} + h_1 \sin \theta_s}{c}} \boldsymbol{\rho}(h_{s,i}) \odot \mathbf{a}_{\text{terrain}}(h_{s,i}) \odot \mathbf{a}(\theta_s) \tag{24}$$

Therefore, the signal model of the whole array can be written as Equation (25).

Finally, we need to discuss the horizontal distance of the reflection point, because the ground of the reflection point directly determines the reflection coefficient. First, from Figure 4, we can see that the reflection points of each array element are inconsistent, which is a function of the elevation angle θ_s of the incident reflected wave and the height $h_{s,i}$ of the reflection point. The horizontal distance of the reflection point of each array element can be calculated by simple trigonometric function as $(h_i + h_{s,i}) \tan \theta_s$.

$\mathbf{x}(t)$

$$\begin{aligned}
 &= \bar{\mathbf{x}}_d(t) + \bar{\mathbf{x}}_s(t) + \mathbf{n}(t) \\
 &= s(t)e^{-j2\pi f \frac{\bar{R}_{d,1}}{c}} \mathbf{a}(\theta_d) \\
 &\quad + s(t)e^{-j2\pi f \frac{\bar{R}_{s,1}}{c}} \boldsymbol{\rho}(h_{s,i}) \odot \mathbf{a}_{\text{terrain}}(h_{s,i}) \odot \mathbf{a}(\theta_s) + \mathbf{n}(t) \\
 &= \left[\mathbf{a}(\theta_d) + e^{-j2\pi f \frac{\bar{R} + h_1 \sin \theta_s - \bar{R}_{d,1}}{c}} \boldsymbol{\rho}(h_{s,i}) \odot \mathbf{a}_{\text{terrain}}(h_{s,i}) \odot \mathbf{a}(\theta_s) \right] \\
 &\quad \cdot s(t)e^{-j2\pi f \frac{\bar{R}_{d,1}}{c}} + \mathbf{n}(t) \\
 &= \left[\mathbf{a}(\theta_d) + e^{-j\delta} \boldsymbol{\rho}(h_{s,i}) \odot \mathbf{a}_{\text{terrain}}(h_{s,i}) \odot \mathbf{a}(\theta_s) \right] \\
 &\quad \cdot s(t)e^{-j2\pi f \frac{R_{d,1}}{c}} + \mathbf{n}(t) \tag{25}
 \end{aligned}$$

The wave path difference in Equation (25) is defined as:

$$\delta = 2\pi f \frac{2h_1 h_t}{cR} \tag{26}$$

It should be noted that the wave path difference in Equation (26) is not the real wave path difference, and the influence $\mathbf{a}_{\text{terrain}}(h_{s,i})$ needs to be added. Obviously, when the terrain has no undulation, $\mathbf{a}_{\text{terrain}}(h_{s,i})$ becomes a vector with constant 1, and Equation (25) degenerates into the mirror reflection model of Equation (9).

V. PRECISE HEIGHT MEASUREMENT MODEL OF MIMO RADAR IN COMPLEX TERRAIN

Above, we have established the signal receiving model of complex terrain. However, unlike the traditional meter wave radar, the meter wave MIMO radar signal has four transmission channels. So in this section, we extend it to meter wave MIMO array radar. The signal model of four transmission paths corresponding to one target of meter wave MIMO radar is shown in Figure 5.

From Figure 5, we can clearly see the four transmission paths of the meter wave MIMO radar. Then the two paths in Equation (25) are extended to the four paths. For MIMO radar, the signal model after matched filtering is Kronecker product of transmitted and received signals. This has been deduced in previous meter wave MIMO radar [13], [14], it is

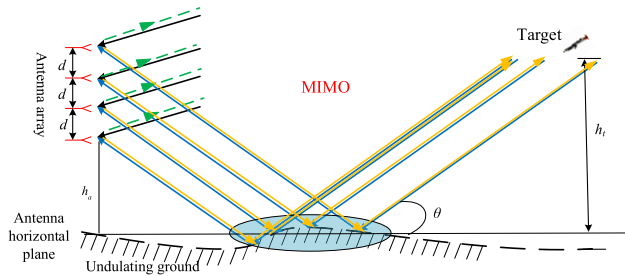


FIGURE 5. Reflection model of complex terrain in low elevation of meter wave MIMO radar.

extended to the form of complex terrain, as follows.

$$\begin{aligned} \mathbf{x}_{\text{mimo}}(t) &= \left[\mathbf{a}_t(\theta_d) + e^{-j\delta} \boldsymbol{\rho}(h_{s,i}) \odot \mathbf{a}_{\text{terrain}}(h_{s,i}) \odot \mathbf{a}_t(\theta_s) \right] \\ &\otimes \left[\mathbf{a}_r(\theta_d) + e^{-j\delta} \boldsymbol{\rho}(h_{s,i}) \odot \mathbf{a}_{\text{terrain}}(h_{s,i}) \odot \mathbf{a}_r(\theta_s) \right] s(t) \\ &+ \mathbf{n}_{\text{mimo}}(t) \end{aligned} \quad (27)$$

In this signal model, it is assumed that the transmitting and receiving elements are shared, that is, the transmitter and receiver are co-located. Then, we have

$$\begin{cases} \mathbf{a}_t(\theta_d) = \mathbf{a}_r(\theta_d) = \mathbf{a}(\theta_d) \\ \mathbf{a}_t(\theta_s) = \mathbf{a}_r(\theta_s) = \mathbf{a}(\theta_s) \end{cases} \quad (28)$$

It is usually assumed that the noise $\mathbf{n}_{\text{mimo}}(t) \in \mathbb{C}^{M^2 \times 1}$ is white noise. The height measurement task of meter wave MIMO radar is to calculate the parameters θ_d according to the received data in Equation (27).

VI. METER WAVE MIMO RADAR HEIGHT MEASUREMENT BASED ON MAXIMUM LIKELIHOOD AND GENERALIZED MUSIC UNDER THE PRECISE SIGNAL MODEL

The before results show that the relationship between ‘‘coherent signal’’ and ‘‘multipath signal’’ in conventional phased array can be basically the same. All the effective algorithms for coherent signal processing can be applied to multipath signal, such as the classical spatial smoothing decoherence algorithm. However, the relationship between ‘‘coherent signal’’ and ‘‘multipath signal’’ in MIMO radar is not equivalent. Because of the mutual penetration of signals in MIMO radar, the traditional spatial smoothing cannot be used, and the traditional subspace based classical super-resolution algorithms ESPRIT and MUSIC cannot be used directly. Therefore, super-resolution algorithms such as maximum likelihood algorithm and generalized MUSIC algorithm without decoherence are fully used in MIMO radar height measurement. The application of these two algorithms in meter wave MIMO radar is briefly reviewed.

A. MAXIMUM LIKELIHOOD

Maximum likelihood estimation is one of the most common and effective parameter estimation methods in array signal

processing. It can be seen from the parameter selection criteria that the algorithm is not affected by the correlation between signals.

Firstly, the signal source and steering vector in the received data of MIMO radar in Equation (27) are recombined into the following form:

$$\begin{aligned} &\left[\mathbf{a}_t(\theta_d) + e^{-j\delta} \boldsymbol{\rho}(h_{s,i}) \odot \mathbf{a}_t(h_{s,i}) \odot \mathbf{a}_t(\theta_s) \right] \\ &\otimes \left[\mathbf{a}_r(\theta_d) + e^{-j\delta} \boldsymbol{\rho}(h_{s,i}) \odot \mathbf{a}_r(h_{s,i}) \odot \mathbf{a}_r(\theta_s) \right] s(t) \\ &= \left[\mathbf{a}_t(\theta_d) \boldsymbol{\rho}(h_{s,i}) \odot \mathbf{a}_t(h_{s,i}) \odot \mathbf{a}_t(\theta_s) \right] \\ &\otimes \left[\mathbf{a}_r(\theta_d) \boldsymbol{\rho}(h_{s,i}) \odot \mathbf{a}_r(h_{s,i}) \odot \mathbf{a}_r(\theta_s) \right] \begin{bmatrix} 1 \\ e^{j\delta} \\ e^{j\delta} \\ e^{j2\delta} \end{bmatrix} s(t) \end{aligned} \quad (29)$$

Then, the received data in Equation (27) can be written as follows:

$$\mathbf{x}_{\text{mimo}}(t) = \mathbf{A}_{\text{mimo}}(\theta_d, \theta_s, h_{s,i}) \bar{\mathbf{s}}(t) + \mathbf{n}_{\text{mimo}}(t) \quad (30)$$

where

$$\begin{aligned} \mathbf{A}(\theta_d, \theta_s, h_{s,i}) &= \left[\mathbf{a}_t(\theta_d) \boldsymbol{\rho}(h_{s,i}) \odot \mathbf{a}_t(h_{s,i}) \odot \mathbf{a}_t(\theta_s) \right] \\ &\otimes \left[\mathbf{a}_r(\theta_d) \boldsymbol{\rho}(h_{s,i}) \odot \mathbf{a}_r(h_{s,i}) \odot \mathbf{a}_r(\theta_s) \right] \in \mathbb{C}^{M^2 \times 4} \end{aligned} \quad (31)$$

We define the equivalent signal vector as follows.

$$\bar{\mathbf{s}}(t) = \begin{bmatrix} 1 \\ e^{j\delta} \\ e^{j\delta} \\ e^{j2\delta} \end{bmatrix} s(t) \quad (32)$$

For detailed derivation, please refer to the formula (5.2.10) on page 148 of Reference [24]. The maximum likelihood estimation criterion can be expressed as follows:

$$\hat{\boldsymbol{\theta}} = - \arg \max_{\boldsymbol{\theta}} \text{tr} \left[\mathbf{P}_{\mathbf{A}(\boldsymbol{\theta})} \hat{\mathbf{R}}_{\text{mimo}} \right] \quad (33)$$

where $\hat{\boldsymbol{\theta}}$ is the maximum likelihood estimation of $\boldsymbol{\theta}$, $\mathbf{A}(\boldsymbol{\theta})$ is the steering vector matrix, $\hat{\mathbf{R}}_{\text{mimo}}$ is the estimated covariance matrix of the array output signal, $\mathbf{P}_{\mathbf{A}(\boldsymbol{\theta})}$ is the projection matrix of the column vector projected into the space of the steering vector matrix $\mathbf{A}(\boldsymbol{\theta})$, and its value is equal to:

$$\mathbf{P}_{\mathbf{A}(\boldsymbol{\theta})} = \mathbf{A}(\boldsymbol{\theta}) \left[\mathbf{A}^H(\boldsymbol{\theta}) \mathbf{A}(\boldsymbol{\theta}) \right]^{-1} \mathbf{A}^H(\boldsymbol{\theta}) \quad (34)$$

According to the above definition, it can be seen that for MIMO array radar, the maximum likelihood in Equation (33) $\boldsymbol{\theta} = [\theta_d \theta_s, h_{s,i}]$ is the direct wave, reflected wave and field fluctuation parameters of the source. The steering matrix and signal covariance matrix in Equation (33) are as follows:

$$\begin{cases} \mathbf{A}(\boldsymbol{\theta}) = \mathbf{A}_{\text{mimo}}(\theta_d, \theta_s, h_{s,i}) \\ \hat{\mathbf{R}}_{\text{mimo}} = E \left\{ \mathbf{x}_{\text{mimo}}(t) \mathbf{x}_{\text{mimo}}(t)^H \right\} \end{cases} \quad (35)$$

TABLE 1. Orthogonality of “steering vector”, “steering matrix” and “noise subspace”.

	Conventional array radar	MIMO array radar
	Noise subspace	Noise subspace
Steering vector	Orthogonal (MUSIC)	Not orthogonal (MUSIC)
Steering matrix (Signal subspace)	Orthogonal (generalized MUSIC)	Orthogonal (generalized MUSIC)

B. GENERALIZED MUSIC

Traditional MUSIC algorithm is based on the orthogonality of signal subspace and noise subspace. However, in MIMO radar, due to the influence of coherent signal, the steering vector is not orthogonal to the noise subspace. Even if a certain method is used to decoherence, the steering vector signals penetrate each other, which leads to the fact that the steering vector is not orthogonal to the noise subspace, so the traditional MUSIC algorithm cannot be directly applied. The generalized MUSIC is also based on the orthogonality of signal subspace and noise subspace. But it does not use the steering vector, but uses the principle that the steering matrix is orthogonal to the noise subspace. In this paper, we need to pay attention to the relationship among “steering vector”, “steering matrix” and “noise subspace”, as shown in Table 1.

It can be clearly seen from the above table that traditional MUSIC is not available for MIMO array radar, while generalized MUSIC is available. The noise subspace E_n and signal subspace E_s are obtained by eigendecomposition of the covariance matrix \hat{R}_{mimo} of matched filtered MIMO array radar. According to the derivation of Reference [4], the generalized MUSIC spectrum is as follows:

$$P(\theta) = \frac{\det [A_{mimo}(\theta_d, \theta_s, h_{s,i})^H A_{mimo}(\theta_d, \theta_s, h_{s,i})]}{\det [A_{mimo}(\theta_d, \theta_s, h_{s,i})^H E_n E_n^H A_{mimo}(\theta_d, \theta_s, h_{s,i})]} \tag{36}$$

where $\det [\cdot]$ is to find its determinant.

C. DIMENSION REDUCTION PROCESSING

Both the maximum likelihood Equation (33) and the generalized MUSIC Equation (35) involve multidimensional search. This amount of calculation is not acceptable in engineering, so it needs to be reduced the searching dimension. Firstly, the geometric relationship between direct wave and reflected wave can be used to reduce the dimension, as follows.

$$\theta_s = -\arcsin(\sin \theta_d + 2h_a/R) \tag{37}$$

In addition, in the following simulation, some assumptions are made to further reduce the searching dimension. One is to assume that the height of terrain relief is known, that is

the parameters $h_{s,i}, i = 1, \dots, M$ are known. Second, when calculating the reflection coefficient, the dielectric constant ϵ_r and surface material conductivity σ_e of the reflection coefficient are known, and the calculation formula of the reflection coefficient is as follows [26].

$$\rho(\theta_d, h_{s,i}) = \frac{\sin \theta_d - \sqrt{\epsilon(h_{s,i}) - \cos^2 \theta_d}}{\sin \theta_d + \sqrt{\epsilon(h_{s,i}) - \cos^2 \theta_d}} \tag{38}$$

$\epsilon(h_{s,i})$ is the surface complex permittivity, which can be expressed by relative permittivity and surface material conductivity:

$$\epsilon(h_{s,i}) = \epsilon_r(h_{s,i}) - j60\lambda\sigma_e(h_{s,i}) \tag{39}$$

The dielectric constant $\epsilon_r(h_{s,i})$ and surface material conductivity $\sigma_e(h_{s,i})$ of different ground surfaces can be found in Reference [26]. In fact, we cannot get the reflection coefficient accurately. Therefore, it needs other more robust angle estimation algorithms, but this is not the focus of the paper.

VII. COMPUTER SIMULATIONS

The number of transmitting elements of meter wave MIMO array radar equals $M = 10$, the array element spacing is half wavelength. The incident frequency is 300MHz, then the incident wavelength is $\lambda = 1$ m, the target direct wave angle is set as $\theta_d = 6$ degrees, then the reflection angle can be calculated according to Equation (37). The antenna height is $h_a = 5$ m, and the target height is $h_t = 3000$ m.

The complex terrain is set as follows. The reflection coefficient is set to two parts. The first one corresponding to the first half array is set the dielectric constant and surface material conductivity equal $\epsilon_r = 80$ and $\sigma_e = 0.2$. The second one corresponding to the second half array is set the dielectric constant and surface material conductivity equal $\epsilon_r = 75$ and $\sigma_e = 0.5$. The fluctuation of the complex terrain in the reflection area is set as $h_{s,i,i=1,\dots,M} = [0.10.20.30.40.50.50.40.30.20.1]^T$.

Example 1 (Spatial Spectrum): The SNR is set as SNR = 20 dB. The number of snapshots is set to 10. In Figures 6 and Figure 7, the terrain matching algorithms based on generalized MUSIC and maximum likelihood estimation are given, and the simulation results of terrain mismatch caused by complex terrain are given respectively. In the following figures, terrain matching algorithms based on maximum likelihood and generalized MUSIC are marked with Match ML and Match G-MUSIC, respectively. Terrain mismatching algorithms based on maximum likelihood and generalized MUSIC are marked with Mismatch ML and Mismatch G-MUSIC, respectively. We can see that the matching algorithms can correctly estimate the real angle value, but the spectrum peak of the mismatch algorithm has shifted.

Example 2 (Results of RMSE Varying With SNR for Elevation and Height Estimation): The root mean square

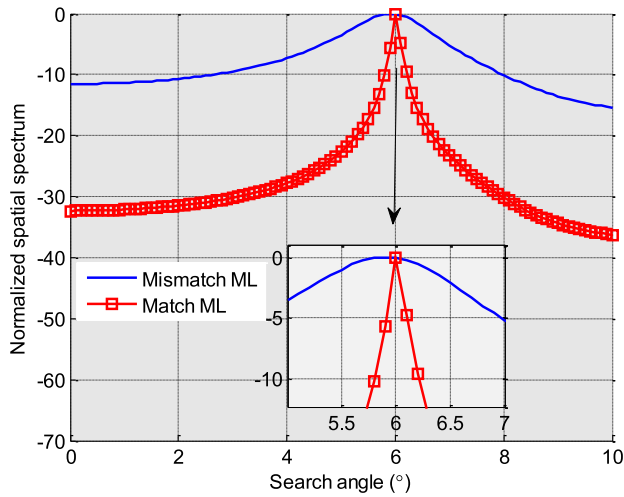


FIGURE 6. Maximum likelihood results.

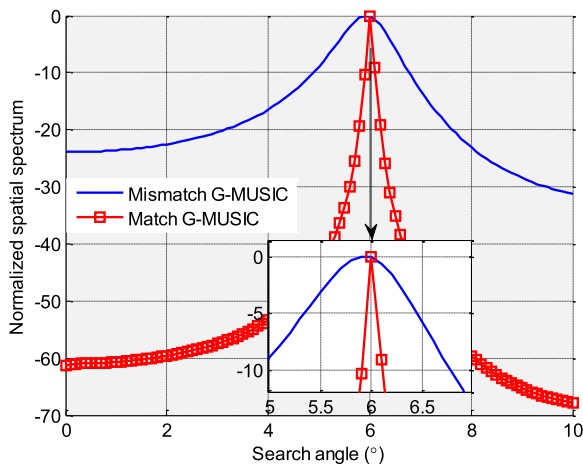


FIGURE 7. Generalized MUSIC results.

error (RMSE) of estimation results is defined as:

$$RMSE = \sqrt{\frac{1}{Monte} \sum_{p=1}^{Monte} E[(\hat{\alpha}_p - \alpha_p)^2]} \quad (40)$$

where $\hat{\alpha} = \hat{\theta}_d$ is the direct wave angle estimation value, $\alpha = \theta_d$ is the real target angle value. When the target height is estimated, the parameter denote $\hat{\alpha} = \hat{h}_t$, and $\alpha = h_t$ is the real value of the target height. 1000 Monte Carlo experiments runs. The number of snapshots is set to 10. The SNR changes from 0 to 25 dB. The angle estimation RMSE and height measurement RMSE of maximum likelihood and generalized MUSIC algorithm are given in Figures 8 and 9. It can be seen from the figure that these two algorithms can be correctly applied in the field of MIMO radar height measurement. The estimation accuracy of the matching algorithm is reduced with the increase of SNR, it is an unbiased estimation. The estimation accuracy of the mismatch algorithm cannot be reduced with the increase of SNR, it is a biased estimation.

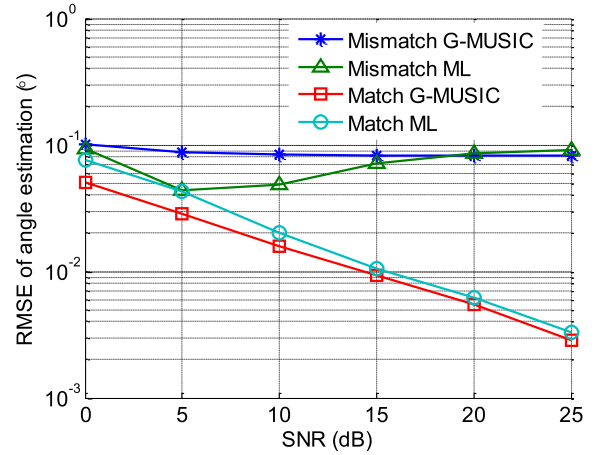


FIGURE 8. Angle estimation RMSE of maximum likelihood and generalized MUSIC algorithm.

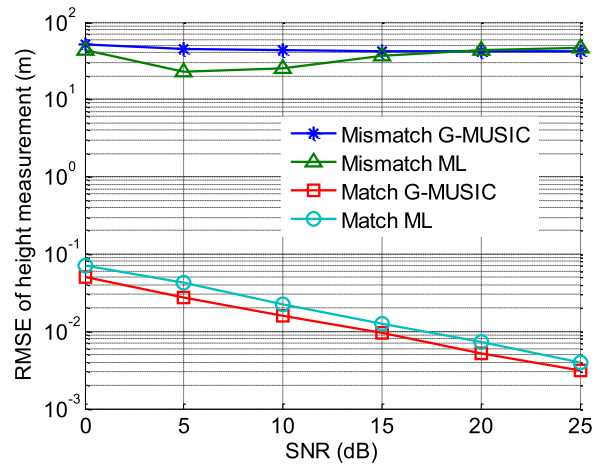


FIGURE 9. Height measurement RMSE of maximum likelihood and generalized MUSIC algorithm.

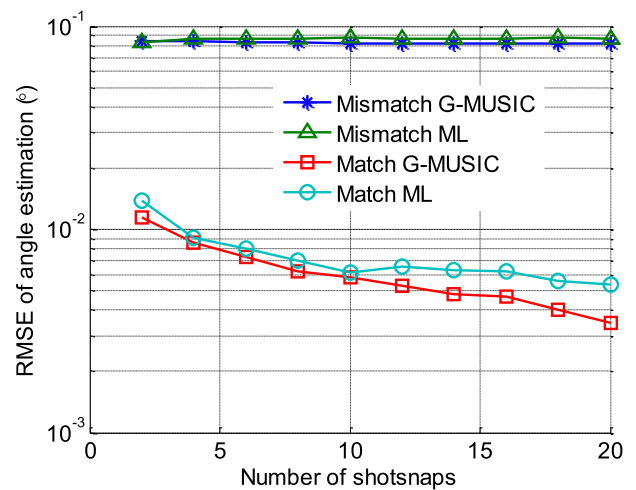


FIGURE 10. Angle estimation RMSE of maximum likelihood and generalized MUSIC algorithm.

Example 3 (Results of RMSE of Elevation and Height Estimation Varying With the Number of Snapshots): The SNR is set as SNR = 20 dB. The number of snapshots is set

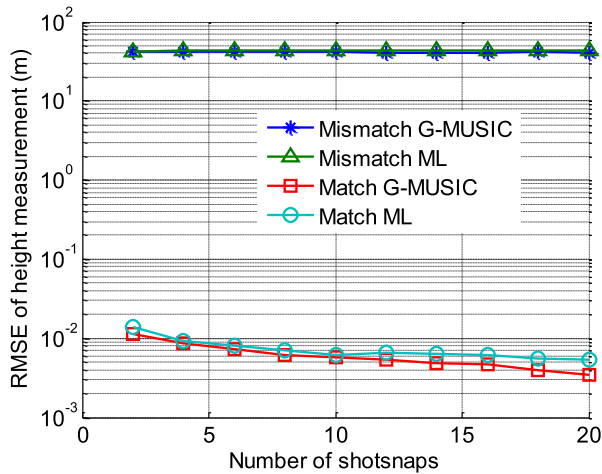


FIGURE 11. Height measurement RMSE of maximum likelihood and generalized MUSIC algorithm.

as from 2 to 20. The angle estimation RMSE and height measurement RMSE of maximum likelihood and generalized MUSIC algorithm are given in Figures 10 and 11. It can be seen from the figures that it has the similar conclusion to that of example 2.

VIII. SUMMARY

Aiming at the problem of meter wave radar height measurement, the author realizes that the reflection signal model of the ground is the key point of height measurement problem, points out the problem of simplifying the reflection point of the flat ground model, and gives the calculation of the horizontal ground of the reflection point, so that the reflection coefficient of each array element can be obtained accurately, which is more accurate than the original model. Secondly, for the undulating ground, the traditional reflection model mismatch is serious, which greatly affects the accuracy of height measurement. In this paper, the closed form calculation of the wave path difference and the height of each reflection point are given. The accurate reflection steering vector is obtained, and the calculation formula of the reflection point ground is given. It is extended to MIMO radar, and then two corresponding height measurement algorithms are given. Simulation results show that the algorithm of surface terrain matching is better than the estimation of terrain mismatch algorithm.

ACKNOWLEDGMENT

This article was presented in part at the 2020 IEEE 3rd International Conference on Electronic Information and Communication Technology, Shenzhen, China, November 13–15, 2020.

REFERENCES

- [1] H. Kuschel, "VHF/UHF radar. Part 1: Characteristics," *Electron. Commun. Eng. J.*, vol. 14, no. 2, pp. 61–72, Apr. 2002.
- [2] H. Kuschel, "VHF/UHF radar. Part 2: Operational aspects and applications," *Electron. Commun. Eng. J.*, vol. 14, no. 3, pp. 101–111, Jun. 2002.
- [3] B. Chen, G. Zhao, and S. Zhang, "Altitude measurement based on beam split and frequency diversity in VHF radar," *IEEE Trans. Aerosp. Electron. Syst.*, vol. 46, no. 1, pp. 3–13, Jan. 2010.
- [4] W. Zhang, Y. Zhao, and S. Zhang, "Altitude measurement of meter-wave radar using the general MUSIC algorithm and its improvement," (in Chinese), *J. Electron. Inf. Technol.*, vol. 29, no. 2, pp. 387–390, 2007.
- [5] Y. Liu, H. Liu, X.-G. Xia, L. Zhang, and B. Jiu, "Projection techniques for altitude estimation over complex multipath condition-based VHF radar," *IEEE J. Sel. Topics Appl. Earth Observ. Remote Sens.*, vol. 11, no. 7, pp. 2362–2375, Jul. 2018.
- [6] S. Huan, M. Zhang, and G. Dai, "Low elevation angle estimation with range super-resolution in wideband radar," *Sensors*, vol. 20, no. 11, p. 3104, 2020.
- [7] J. Li and P. Stoica, "MIMO radar with collocated antennas," *IEEE Signal Process. Mag.*, vol. 24, no. 5, pp. 106–114, Oct. 2007.
- [8] A. Haimovich, R. Blum, and J. Cimini, "MIMO radar with widely separated antennas," *IEEE Signal Process. Mag.*, vol. 25, no. 1, pp. 116–129, Dec. 2008.
- [9] L. Wan, L. Sun, K. Liu, X. Wang, Q. Lin, and T. Zhu, "Autonomous vehicle source enumeration exploiting non-cooperative UAV in software defined Internet of vehicles," *IEEE Trans. Intell. Transp. Syst.*, early access, Sep. 23, 2020, doi: [10.1109/TITS.2020.3018377](https://doi.org/10.1109/TITS.2020.3018377).
- [10] L. Wan, Y. Sun, L. Sun, Z. Ning, and J. J. P. C. Rodrigues, "Deep learning based autonomous vehicle super resolution DOA estimation for safety driving," *IEEE Trans. Intell. Transp. Syst.*, early access, Aug. 21, 2020, doi: [10.1109/TITS.2020.3009223](https://doi.org/10.1109/TITS.2020.3009223).
- [11] J. Shi, G. Hu, B. Zong, and M. Chen, "DOA estimation using multipath echo power for MIMO radar in low-grazing angle," *IEEE Sensors J.*, vol. 16, no. 15, pp. 6087–6094, Aug. 2016.
- [12] J. Shi, G. Hu, and T. Lei, "DOA estimation algorithms for low-angle targets with MIMO radar," *Electron. Lett.*, vol. 52, no. 8, pp. 652–654, Apr. 2016.
- [13] J. Liu, Z. Liu, and R. Xie, "Low angle estimation in MIMO radar," *Electron. Lett.*, vol. 46, no. 23, pp. 1565–1566, Nov. 2010.
- [14] X. Wu, Y. Zhao, S. Zhang, and M. Dong, "New method for DOA estimation for the MIMO radar in low-angle tracking environment," (in Chinese), *J. Xidian Univ.*, vol. 35, no. 5, pp. 793–798, 2008.
- [15] J. Tan and Z. Nie, "Polarisation smoothing generalised MUSIC algorithm with PSA monostatic MIMO radar for low angle estimation," *Electron. Lett.*, vol. 54, no. 8, pp. 527–529, Apr. 2018.
- [16] Y. Liu, B. Jiu, X.-G. Xia, H. Liu, and L. Zhang, "Height measurement of low-angle target using MIMO radar under multipath interference," *IEEE Trans. Aerosp. Electron. Syst.*, vol. 54, no. 2, pp. 808–818, Apr. 2018.
- [17] Y. Liu, H. Wang, and B. JIU, "A new method for DOA estimation for VHF MIMO radar in low-angle tracking environment," (in Chinese), *J. Electron. Inf. Technol.*, vol. 38, no. 3, pp. 622–628, 2016.
- [18] C. Chen, J. Tao, G. Zheng, and Y. Song, "Beam split algorithm for height measurement with meter-wave MIMO radar," *IEEE Access*, vol. 9, pp. 5000–5010, 2021.
- [19] J. Tan, Z. Nie, and S. Peng, "Adaptive time reversal MUSIC algorithm with monostatic MIMO radar for low angle estimation," in *Proc. IEEE Radar Conf. (RadarConf)*, Boston, MA, USA, Apr. 2019, pp. 1–6.
- [20] J. Liu, Z. Liu, R. Xie, and Y. F. Liu, "Beam-space domain angle estimation algorithm in VHF MIMO radar," (in Chinese), *Acta Electronica Sinica*, vol. 39, no. 9, pp. 1961–1966, 2011.
- [21] R. Xie, Z. Liu, and J. Liu, "Fast algorithm for low elevation estimation based on matrix pencil in MIMO radar," (in Chinese), *J. Electron. Inf. Technol.*, vol. 33, no. 8, pp. 1833–1838, 2011.
- [22] S. Wang, Y. Cao, H. Su, and Y. Wang, "Low angle estimation for MIMO radar with arbitrary array structures," *Int. J. Electron. Lett.*, vol. 7, no. 4, pp. 422–433, Oct. 2019.
- [23] Y. Song, G. Hu, and G. Zheng, "Refined signal model of meter wave radar for height measurement under complex terrain," in *Proc. IEEE 3rd Int. Conf. Electron. Inf. Commun. Technol. (ICEICT)*, Shenzhen, China, Nov. 2020, pp. 520–524.
- [24] Y. Wang, H. Chen, Y. Peng, and Q. Wan, *Theory and Method of Spatial Spectrum Estimation*. Beijing, China: Tsinghua Univ. Press, 2004.
- [25] R. F. Harrington, *Time Harmonic Electromagnetic Fields*. New York, NY, USA: McGraw-Hill, 1961.
- [26] J. Wu, *Advanced Metric Wave Radar*. Springer, 2020.



YUWEI SONG was born in Liaoning, China, in 1986. She received the B.Eng. degree in biomedical engineering and M.Eng. degree in circuit and system from Xidian University, China, in 2009 and 2012, respectively. She is currently pursuing the Ph.D. degree with a focus on direction finding for MIMO radar and vector sensor array radar. From 2012 to 2019, she was an Engineer with Huawei Technology Company Ltd.



GUIMEI ZHENG was born in Fujian, China, in 1987. He received the B.Eng. degree in biomedical engineering and the Ph.D. degree in signal and information processing from Xidian University, China, in 2009 and 2014, respectively. He was with the Department of Electronic Engineering, Tsinghua University, Beijing, China, as a full-time Postdoctoral Research Fellow, from 2015 to 2017. He is currently an Associate Professor with the Air and Missile Defense College, Air Force Engineering University, Xi'an, China. His research interests include MIMO radar and vector sensor array signal processing.

• • •



and image processing.

GUOPING HU graduated from the Air and Missile Defense College, Xi'an, China, in 1985. He received the M.S. degree from the Air and Missile Defense College, in 1990 and the Ph.D. degree in electrical engineering from Xidian University, Xi'an, in 2010. He is currently a Professor and the Director of the Institute of Radar Anti-stealth Technology, Air Force Engineering University. His research interests include radar signal processing, radar anti-stealth technology, wireless communication technology, and image processing.